Geophys. J. Int. (2000) **141,** 539–557

An alternative interpretation of the Cayman trough evolution from a reidentification of magnetic anomalies

S. Leroy,[1] A. Mauffret,[1] P. Patriat[2] and B. Mercier de Lépinay[3]

[1] *Department of Géotectonique, CNRS ESA* 7072, *University of P & M Curie,* 4 *place Jussieu,* 75252 *Paris Cedex* 05, *France. E-mail: sylvie.leroy@lgs.jussieu.fr*

[2] *Institut de Physique du Globe, Case* 89, 4 *place Jussieu,* 75252 *Paris Cedex* 05, *France*

[3] *UMR Geoazur, Sophia Antipolis, rue Albert Einstein,* 06 *Valbonne, France*

Accepted 1999 October 29. Received 1999 October 29; in original form 1998 March 25

SUMMARY

Magnetic data were collected during the Wilkes (1973) and Seacarib II (1987) cruises to the Cayman trough. A new interpretation of magnetic data is carried out. An isochron pattern is drawn up from our anomaly identifications. An early Eocene age (49 Ma, Ypresian) for Cayman trough opening is proposed instead of the late Oligocene or middle Eocene ages suggested by previous studies. Our plate tectonic reconstruction is simpler and fits the on-land geology (Jamaica and Cuba) and the tectonics. Our reconstruction shows a southward propagation of the spreading centre between magnetic anomalies 8 and 6 (26 and 20 Ma). The trough width increases by 30 km in this period. The southward propagation of the Cayman spreading centre from the Middle Oligocene to the Early Miocene induced the development of the restraining bend of the Swan Islands, the formation of a 1 km high scarp on the eastern trace of the Cayman trough transform fault (Walton fault) and the formation of a pull-apart basin (Hendrix pull-apart). Magnetic anomalies and magnetization maps give information about the deformation and the rocks. The proposed evolutionary model of the Cayman trough from the inception of seafloor spreading to the present configuration is presented in relation to the tectonic escape of the northern boundary of the Caribbean plate from the Maastrichtian to the Present.

Key words: geodynamics, magnetic anomaly, North Caribbean plate boundary.

INTRODUCTION

The northern Caribbean plate boundary is located along the Cayman trough. This boundary consists of a 100–250 km wide seismogenic zone of mainly left-lateral strike-slip deformation extending over 2000 km along the northern edge of the Caribbean sea. This left-lateral strike-slip displacement is related to the eastward motion of the Caribbean plate relative to the North America plate (Molnar & Sykes 1969; Jordan 1975) (Fig. 1). The Cayman trough is a long depression that extends from the Belize margin to the northern edge of Jamaica. The geological and geophysical data suggest that the trough is underlain by oceanic crust accreted along a short north–south spreading centre (CAYTROUGH 1979) located between two transform faults: the Oriente (in the north) and Swan (in the south) fault zones. Several attempts to quantify the rate of spreading (Holcombe *et al.* 1973; Macdonald & Holcombe 1978; Holcombe & Sharman 1983; Rosencrantz & Sclater 1986; Rosencrantz *et al.* 1988; Ramana *et al.* 1995) have suggested opening of the trough at an estimated rate of 20 mm yr^{-1} for the period 0–2.4 Ma, but the older opening rates are controversial. Seismicity data (Sykes *et al.* 1982; Mann *et al.* 1995), field mapping in Jamaica (Burke *et al.* 1980; Wadge & Dixon 1984; Mann *et al.* 1985; Pisot 1989), swath mapping (Rosencrantz & Mann 1991) and seismic reflection data (Leroy *et al.* 1996) indicate that the southeastern edge of the Cayman trough has been reactivated since the Miocene along the Walton fault, several faults in Jamaica and the Enriquillo fault in Haiti (Fig. 1). The rate of motion is estimated to be 4 mm yr^{-1} in Jamaica (Burke *et al.* 1980; Mann *et al.* 1985) and 8 mm yr^{-1} in Haiti (Mocquet & Aggarwal 1983).

In this paper, we propose an alternative evolution of the Cayman trough based on a systematic study of the existing bathymetric and magnetic data relative to the structural analyses based on the multichannel seismic reflection data and swath bathymetry collected on the North Jamaican margin (Leroy *et al.* 1996). The continent–ocean transition has been located accurately with these new data. Furthermore, previous magnetic models (Rosencrantz *et al.* 1988; Ramana *et al.* 1995) did not match the geology described on land. The Cayman trough represents a key area for understanding the tectonic framework of the northern Caribbean basin. Thus, it is important to

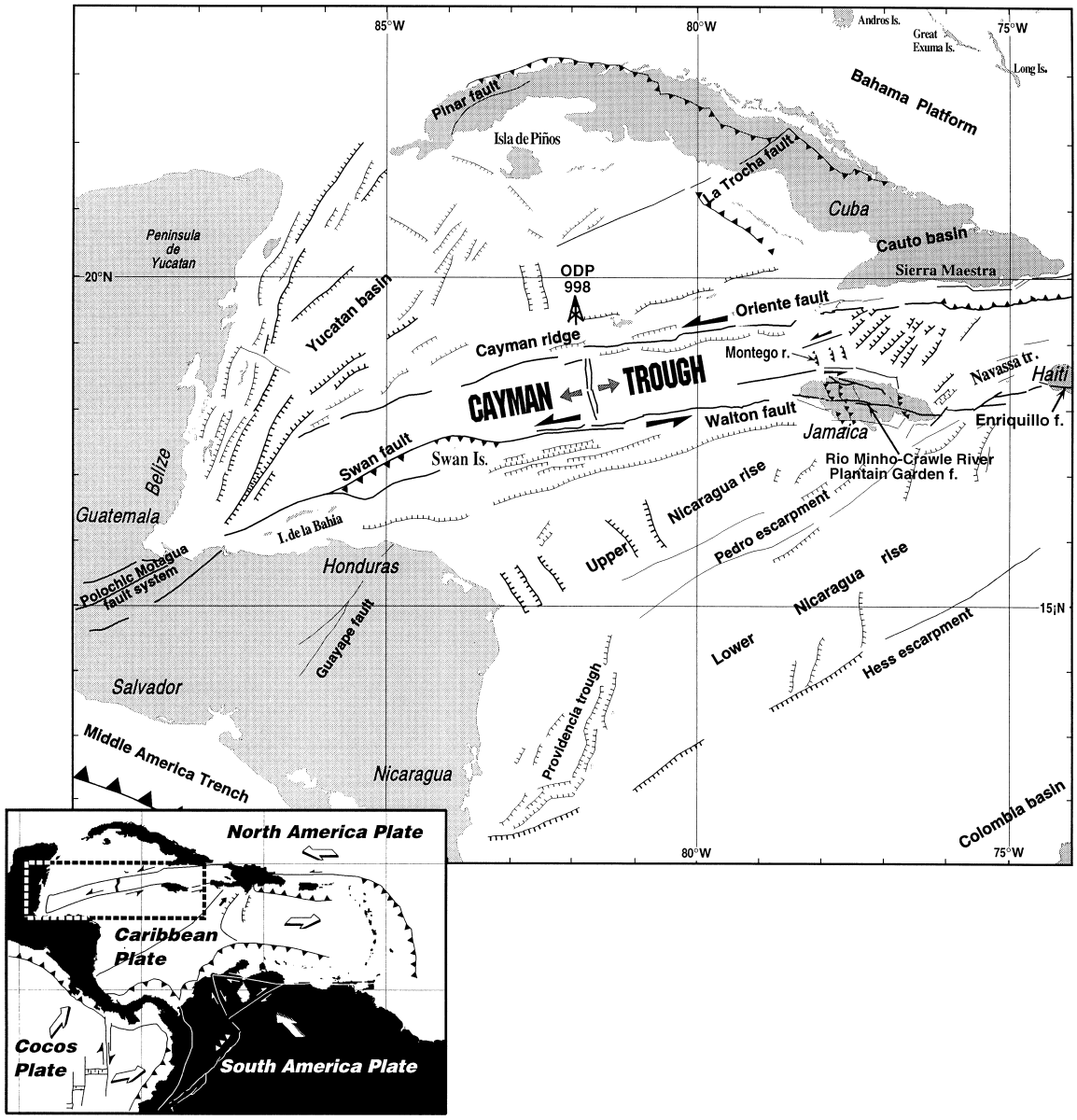

Figure 1. Tectonic sketch of the northern Caribbean domain showing the major geographic provinces and the dominant fault patterns.

document the structures along the trough using bathymetry and to determine the onset of seafloor spreading using magnetic anomalies.

BATHYMETRIC STUDY

An accurate study of the Eastern Cayman trough has been presented previously (Leroy *et al.* 1996); here we broaden this study to the entire Cayman trough. Fig. 2 shows the bathymetric map obtained from all of the data available in this zone from the National Geophysical Data Centre, including the multibeam data recording during the Seacarib II cruise in 1987 (Pisot 1989).

The central part of the Cayman trough (between 80°W and 84°W) shows strong relief comprising north–south horsts and graben typical of a spreading centre fabric (Holcombe *et al.* 1973) (Figs 2 and 3a). Indeed, the seafloor deepens both eastwards and westwards on either side of a ridge, the *Mid-Cayman spreading centre*. This N–S spreading axis is very short, being only 150 km long and 30 km wide (Fig. 3). The rift valley is abnormally deep (5500 m average depth with a maximum of 6000 m) and is flanked by rift mountains whose peaks are 2500 m deep. The average strike of the spreading zone is about 080°.

The Mid-Cayman spreading ridge has been classified as a slow or even ultraslow spreading ridge (Holcombe *et al.* 1973; Perfit 1977; CAYTROUGH 1979; Stroup & Fox 1981), similar to a cold 'Atlantic-type' spreading ridge. In these ridges, the neovolcanic zone constitutes the inner valley floor and corresponds to a series of small conical volcanoes (Smith & Cann 1990). The basalt production is weak and peridotite may constitute the basement (CAYTROUGH 1979). Moreover, in the very narrow Cayman trough the heat is diffused along the rift wall (Rosencrantz & Sclater 1986). Global studies in the Pacific and Atlantic oceans have shown that depth and heat flow are functions of the age of the lithosphere (Parsons &

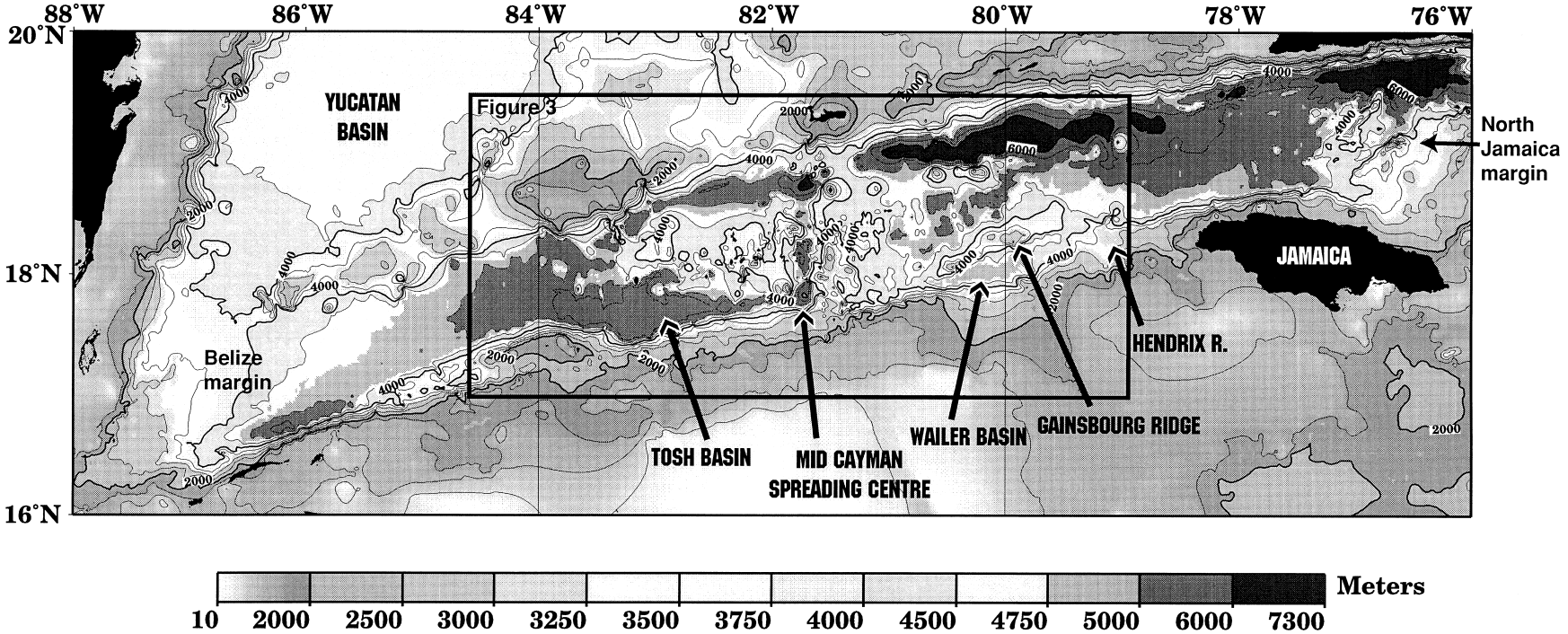

Figure 2. Bathymetric map of the Cayman trough. Depths are in metres and the contour interval is 500 m. Several morphological features are recognized from west to east: the Yucatan basin, the Tosh basin, the Mid-Cayman spreading centre, the Wailer basin, the Gainsbourg ridge and the Hendrix rhomboidal basin.

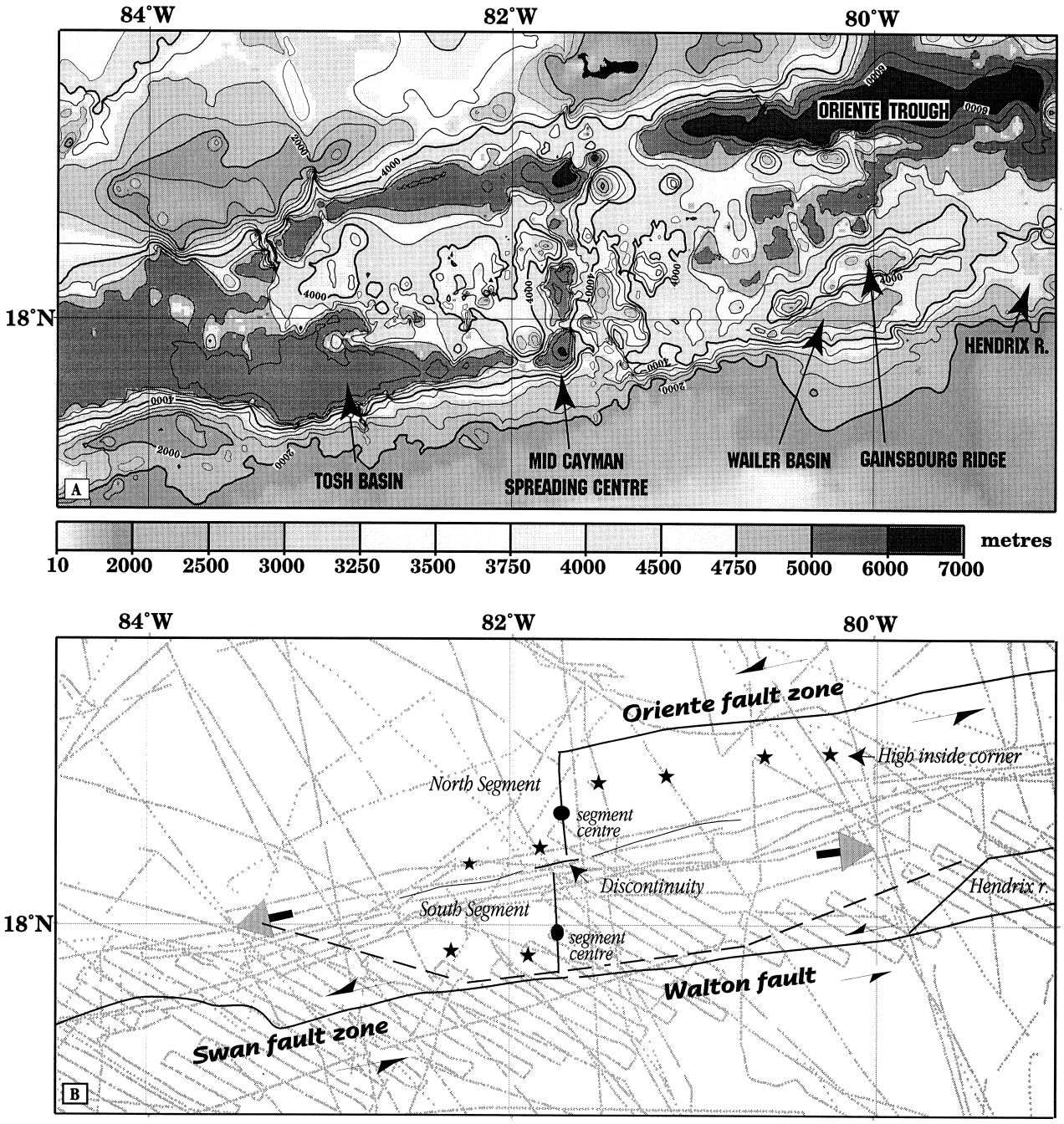

Figure 3. (a) Detailed bathymetric map of the Mid-Cayman spreading centre. Depths are in metres and the contour interval is 500 m. (b) Interpretation of the spreading ridge's morphological features. The grey dotted lines correspond to the shipping tracks used for this study. The dashed line represents the northern boundary of the two nodal basins, the Tosh and Wailer basins.

Sclater 1977). Thus, for ages of less than 80 Myr, the seafloor depth is related to the square root of the lithosphere age and is about 2500 m at zero age (Sclater & Francheteau 1970; Parsons & Sclater 1977). Analyses of the rift valley depth along the Mid-Atlantic Ridge have revealed some depth anomalies in relation to the theoretical model (Le Douaran & Francheteau 1981). This is also the case for the Mid-Cayman ridge, for which the seafloor is 2 km deeper than the theoretical depth (Rosencrantz & Sclater 1986).

The Mid-Cayman spreading centre (Fig. 3) is formed by two segments, separated by a discontinuity which was interpreted as a transform fault by previous authors (Ladd *et al.* 1990). This discontinuity has a sinistral strike-slip focal mechanism. The segment centre rises to 4200 m and the segments deepen on either side to a maximum of 6100 m southwards and 6500 m northwards. The discontinuity is at a depth of 4500 m. We have determined lengths of 60 km for the northern segment and 70 km for the southern segment and a separation of 150 km between the two transform faults, Oriente and Swan.

The segments are bounded by high inside corners that correspond to bathymetric highs that are apparent northwards on the eastern flank of the spreading centre (Fig. 3). We can

follow these high inside corners to longitude 80°W. On the other hand, southwards, on the eastern and western flanks, it is more difficult to follow these spreading-centre highs. At the foot of the transform faults, the basins are about 6000 m deep (Fig. 3).

The series of horsts and graben extend about 150 km on either side of the spreading centre. Further away, the seafloor topography of the Cayman trough becomes flat, the sedimentary cover thickening towards the Belize margin.

The strike-slip faults (Figs 2 and 3) bounding the Cayman trough are marked by very steep seafloor slopes, ranging from 2000–4000 m on average. These walls are present on the northern and southern sides of the Cayman trough all along its length. They correspond to the marginal ridges characteristic of transform margins. Locally, deep basins (up to 6500 m) emphasize the northern branch, the Oriente fault zone (Oriente trough and Oriente basin). The strike of the northern boundary of the Cayman trough is relatively straight, whereas its southern limit is more sinuous. We observe at about 17°30′N, 83°30′W (Figs 2 and 3) an obvious bend of the Swan fault. The trough width is reduced at this point and also at 18°00′N, 79°00′W, on the eastern side of the ridge, where the trough width decreases from 150 to 75 km (Figs 2 and 3). The width change could be due to the initiation of the second segment of the ridge with an increased magmatic supply. The bend of the Swan fault is more marked westwards, on the Belize side, than eastwards, on the Jamaica side. This shape corresponds to the Swan island restraining bend described by Mann *et al.* (1991). Towards Jamaica, the Walton fault, related to the Rio Minho–Crawle River–Plantain Garden fault crossing Jamaica (Fig. 1), shows a rhomboidal-shaped area between 80°W and 78°W at an average depth of 3000 m (Leroy 1995) (Figs 2 and 3). The 4000 and 2000 m isobath lines in this zone bound the rhomboidal area, known as the Hendrix pull-apart, the northern boundary of which corresponds to the Jamaican continental slope (Fig. 2). At 80°W, on the north of the Hendrix pull-apart, an elongate ridge rises to 2800 m depth. This high, called the Gainsbourg ridge, is bounded by a 4500 m deep depression to the south (Fig. 3). We call this depression the Wailer basin. No morphological element is visible on the western flank of the Mid-Cayman spreading centre, but a low known as the Tosh depression, surrounded by the 5000 m isobath line, lies oblique to the spreading centre axis with the same oblique angle as the Gainsbourg ridge. The northern limits of the Tosh and Wailer basins form a widened V-shape, the apex representing the southern end of the spreading centre (Figs 2 and 3) (Leroy 1995).

On the north of the Cayman trough, the Cayman ridge ranges from 500 to 2000 m depth. This bathymetric high bounds the Yucatan basin of 4550 m maximum depth (Fig. 2). On the south of the Cayman trough, the Upper Nicaragua rise constitutes a broad boundary rising to 500 m.

An evolutionary history must be based on the establishment of a chronology. Thus, the bathymetric study of the Cayman trough should be correlated with the identification of magnetic lineations.

MAGNETIC ANOMALY IDENTIFICATIONS

The magnetic anomaly identifications were made by comparing each magnetic anomaly profile with a 2-D block model. This model uses a magnetic reversal timescale (Table 1a) adapted for the slow spreading ridge. The published magnetic scales have been derived, for the most part, from observations at fast spreading ridges, where a maximum number of events can be identified. Applying these different existing scales to slow spreading rates (half-rate <20 mm yr^{-1}) often leads to very different shapes for the same magnetic anomaly. Furthermore, most of these calculated anomalies do not match the corresponding observed anomaly well. Patriat (1987) has shown that it is possible to obtain models matching both fast and slow spreading ridge observations by slightly changing the relative positions of the proposed reversals. This modified scale can be reinterpolated using the few accurate ages from a given magnetic timescale. In order to take into account these various published magnetic scales, the anomalies chosen for identification correspond to boundaries between reverse and normally magnetized blocks that can easily be identified on any timescale and can thus be assigned an age taken from the chosen scale. The ages of our identified anomalies are presented in Table 1(b) at two of the most frequently used timescales for comparison and discussion.

Magnetic data from both the Seacarib II and the Wilkes surveys, corrected for the 1990 IGRF (IAGA 1985; Langel 1988), are plotted in Fig. 4 along the ship tracks and on the topographic map to better locate anomalies in relation to seafloor relief. The magnetic anomalies and bathymetric profiles are drawn in Fig. 5 to simplify the correlation between these profiles. It is important to remember that in the case of a slow spreading centre such as the Cayman spreading ridge, magnetic anomaly identification is not always easy, owing to the great variability of the characteristic shapes. Furthermore, in the case of the Cayman trough, the amplitudes are low (rarely greater than 100 nT). Thus, the characteristic magnetic anomaly shapes are hardly recognizable here, which makes recognition of certain anomalies questionable. Macdonald & Holcombe (1978) and then Rosencrantz *et al.* (1988) (Fig. 6a) previously revealed the variable shapes of these anomalies. Nevertheless, identification is facilitated by taking into account the magnetic contamination (Tisseau & Patriat 1981) that is introduced by a transitional width between two adjacent blocks of opposite magnetization (Fig. 6b).

The magnetic profiles are individually correlated with the computed magnetic profile. Fig. 6(b) illustrates the comparison between the observed and computed anomalies for several Wilkes cruise profiles (USNS Wilkes, Holcombe *et al.* 1973) and two Seacarib II cruise profiles (R/V Jean Charcot, Sc #68, Sc #70). The Wilkes profiles cross the spreading centre and the Seacarib profiles complete the study eastwards, up to the north Jamaican margin. The density of the magnetic profiles is not the same on either side of the spreading centre; notably, west of A8 only one profile (Wilkes #5) extends up to the Belize continental margin (Figs 5 and 6).

The average half-spreading rates used for modelling the Cayman trough magnetic anomalies are 8.5 mm yr^{-1} from the present to A6, then 10 mm yr^{-1} until A18 time, and finally 7.5 mm yr^{-1} to the margin (Fig. 6b).

The amplitude of the *central magnetic anomaly* (CMA or A1) is lower than that of the magnetic model, but the rift valley, clear on the bathymetric map (Figs 2 and 3) is not taken into account in the model. Therefore, these data permit us to locate the axis easily (Figs 6 and 7). On a slow spreading ridge, the CMA is always clearer on the segment centre than on discontinuities (Sloan & Patriat 1992). This observation is

Table 1. (a) Magnetic timescale of Patriat (1987) reinterpolated by Sloan & Patriat (1992) with three fixed reference points at 3.40, 32.46 and 56.14 Ma corresponding to anomalies 2 A (old), 12 (young) and 24 (old) (Kent & Gradstein 1986), respectively. The bold characters indicate the age and the number of the chosen anomalies. (b) Age of magnetic anomalies given by the timescales of Kent & Gradstein (1986) and Cande & Kent (1995).

(a) Normal Polarity Interval (Ma)

Age (Ma)		Anomaly #	Age (Ma)		Anomaly #	Age (Ma)		Anomaly #	Age (Ma)		Anomaly #
0.00	0.20	1	9.84	10.10		18.25	18.51		29.86	30.14	
0.22	0.48		10.13	**10.24**	**5 o**	18.55	18.81		30.19	30.40	
0.50	0.71	1	10.36	10.42		19.07	19.21	6	31.38	31.65	11
0.90	0.96	J	10.56	10.59		19.25	19.35		31.74	32.11	11
1.64	1.86	2	10.86	10.93		19.39	19.53		32.46	32.96	
2.45	2.88	2 A	11.45	11.51		19.57	19.76		**35.51**	35.70	**13 y**
2.95	3.04		11.76	12.01		19.80	20.00		35.77	36.11	13
3.15	3.37	2 A	12.37	12.43		20.02	**20.26**	**6 o**	37.27	37.46	
3.85	3.95	3	12.70	12.84		20.56	20.86		37.50	37.65	
4.08	4.22		13.09	13.31		21.16	21.61		38.03	38.26	
4.37	4.44		13.58	13.86		21.89	22.07		38.42	38.67	
4.51	4.75	3	14.04	14.34		22.37	22.47		38.72	39.09	
5.69	5.97	**3 A y**	14.56	14.66		22.79	22.97		39.54	40.09	
6.04	6.33	3 A	14.83	14.97		23.05	23.40		40.15	40.33	
6.67	6.80	4	15.20	15.24		23.75	23.93		40.39	40.70	
7.01	7.10		15.42	15.46		24.06	24.32		41.02	41.41	18
7.17	7.57		15.65	15.69		24.61	24.80		41.48	41.86	
7.62	7.66	4	15.90	16.15	5C	25.82	25.93		41.92	**42.32**	**18 o**
8.08	8.40	4 A	16.29	16.38		26.00	26.20		42.99	43.27	
8.50	8.69	4 A	16.55	16.72	5C	26.63	26.81	8	44.21	**45.62**	**20**
8.92	9.00	5	16.92	16.96		26.97	27.09		48.16	**49.82**	**21**
9.05	9.21		17.17	17.39		27.17	**27.92**	**8 o**	51.58	**52.35**	**22**
9.25	9.52		17.44	17.63		28.44	28.96		52.71	52.76	22 A
9.55	9.81		17.86	17.95		29.02	29.44		53.58	53.76	23 A
									53.83	54.57	23

(b) Anomaly #	3 A y	5 o	6 o	8 o	13 y	18 o	20 o	21 o	22 o
Kent & Gradstein (1986)	5.35	10.54	20.45	27.74	35.29	42.73	46.17	50.34	52.62
Cande & Kent (1995)	5.89	10.95	20.13	26.55	33.06	40.13	43.79	47.91	49.71

confirmed for the Wilkes profiles, which are located for a large part over the discontinuity area (Fig. 4). Indeed, the CMA is clearest on the Wilkes #1 profile, which is further from the discontinuity (Fig. 4).

Anomaly 3a (A3a) is easily recognizable and seems to have been undisturbed (Fig. 6b), except for the northern profiles (Wilkes #1 & #3; Fig. 5), whereas *A5* appears sometimes amplified and is sometimes difficult to identify, as is the case in most of the oceans (for example, in the Atlantic ocean; Pariso *et al.* 1996), because of the succession of several adjacent normally magnetized blocks. On profiles Wilkes #2 and #3, A5 shows a very high amplitude on the western flank only (Figs 6 and 7b). Here, A5 is located on a marked topographic high almost 2500 m deep. However, at this depth, the topographic effect alone is not strong enough to explain the high amplitude of the western flank A5. The same phenomenon has been noted in the Atlantic ocean in the SARA zone (Rommevaux 1994).

Anomaly A6, on the eastern flank (profile Wilkes #1), also has a high amplitude and is located on a topographic high (Figs 4 and 5). Before A6 time, the spreading rate was slightly higher (8.5–10 mm yr^{-1}). The topography of the seafloor becomes less rough than near the axis. On the western flank, the last apparent bathymetric scarp before the increase of the sedimentary cover on oceanic crust is located at A6. On the eastern flank, the seafloor is less covered by sediments but appears at the same time to have lower relief than in the vicinity of the axis.

Anomalies A8, *A9* and *A10* on the eastern flank appear grouped together and form only one high-amplitude anomaly obvious on the Wilkes #1, #2, #4 and Sc #68 profiles (Fig. 6b). The same holds for *A11* and *A12*, which is usual. No bathymetric effect could explain this high amplitude (Figs 2 and 6) and the slow spreading rate change is not significant enough to explain these phenomena.

Anomaly A13 has a characteristic shape on either side of the axis (on the Wilkes #2, #4 and Sc #68 profiles for the eastern limb and on Wilkes #5 for the western limb). On the other hand, it is difficult to recognize the expected shape of the *A15–A18 series*, but the identification of the next sequence (from *A20* to *A22*) is clear, with a spreading rate of 7.5 mm yr^{-1} (Fig. 6b) for pre-*A18* time.

Anomaly A22 is situated at the continent–ocean transition, as defined by Leroy *et al.* (1996) from a structural study. This anomaly corresponds to an Early Eocene age (49 Ma, Ypresian).

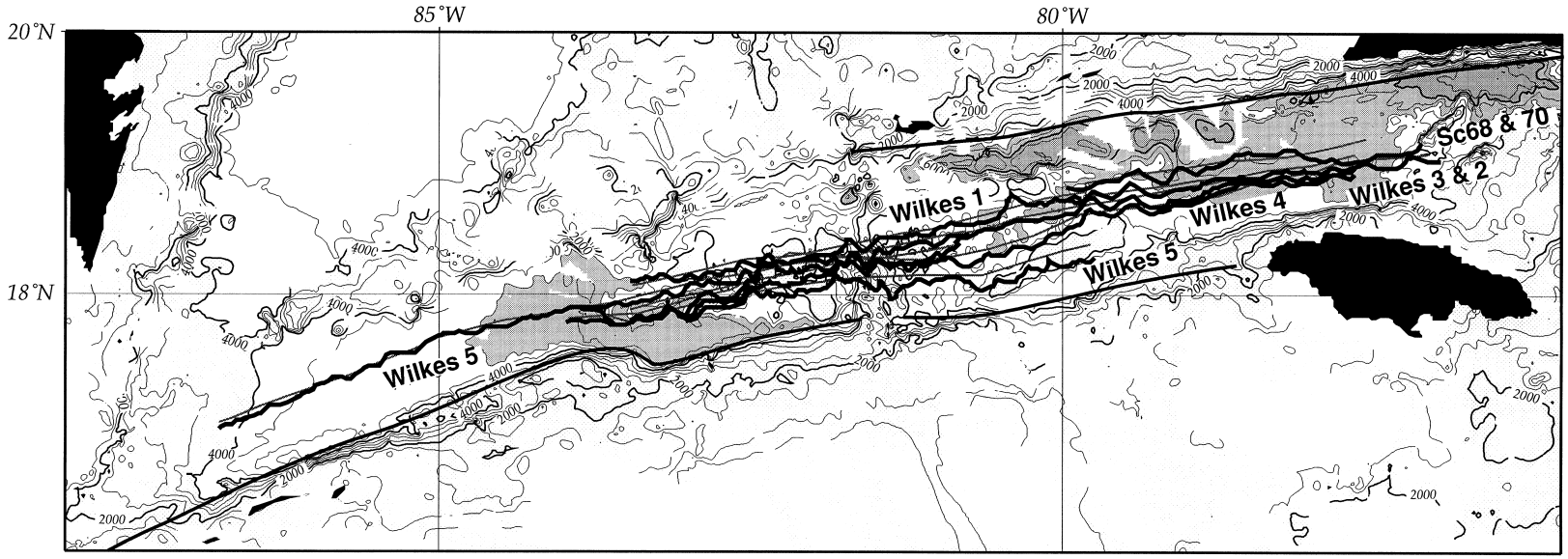

Figure 4. Magnetic anomaly profiles used for our anomaly identifications are projected on to the ship tracks over a bathymetric map. The background bathymetric map shown in Fig. 2 is useful for correlating the magnetic anomalies with the seafloor topography.

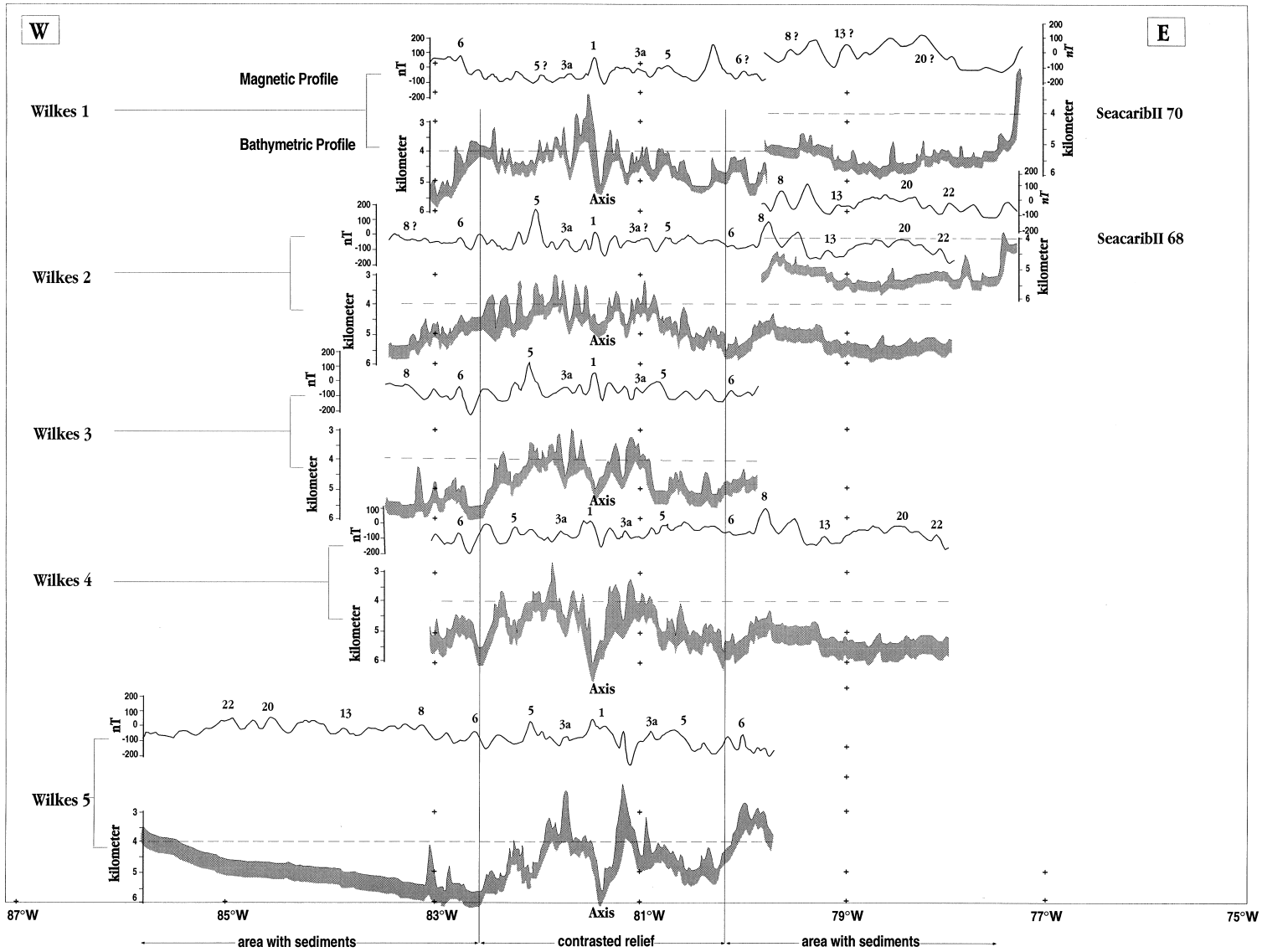

Figure 5. Magnetic and bathymetric profiles of the Cayman trough from the Wilkes and Seacarib II cruises. Profiles are drawn from north to south. Numbers correspond to the magnetic anomalies identified using our model. See Fig. 4 for profile locations.

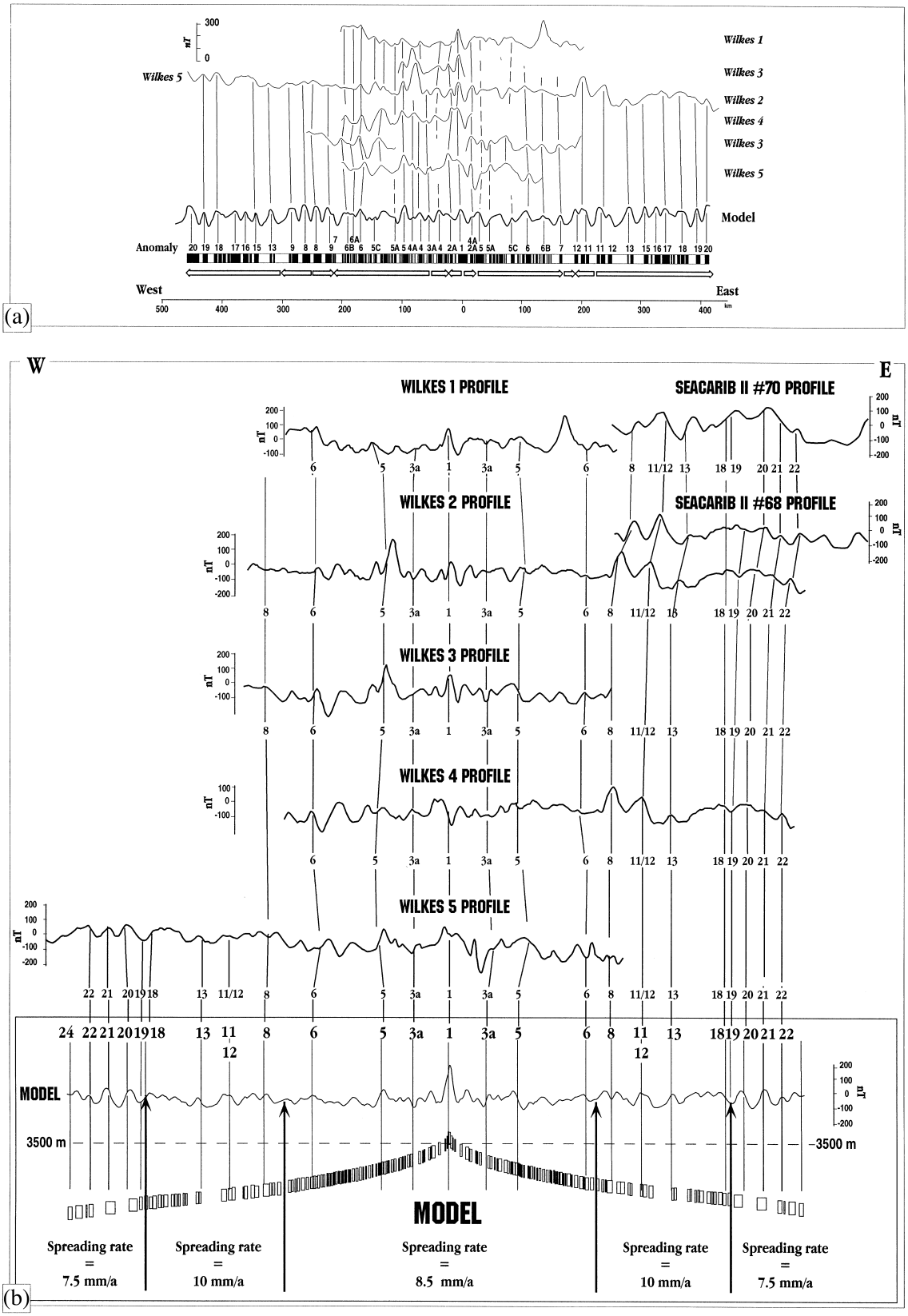

Figure 6. (a) Magnetic model proposed by Rosencrantz *et al.* (1988). (b) Magnetic profiles observed over the Cayman trough (see Fig. 4 for location) and our proposed magnetic model. The spreading rate varies from 7.5 to 10 mm yr^{-1}. The positions of the identified anomalies, indicated by dotted lines, are chosen at the boundaries between certain reversed and normal blocks so that the age of each isochron is defined. Only the normal polarity blocks are shown. We have chosen a magnetic contamination factor of 0.7 (a magnetic contamination factor of 1 being the normal model without contamination; see text for explanation).

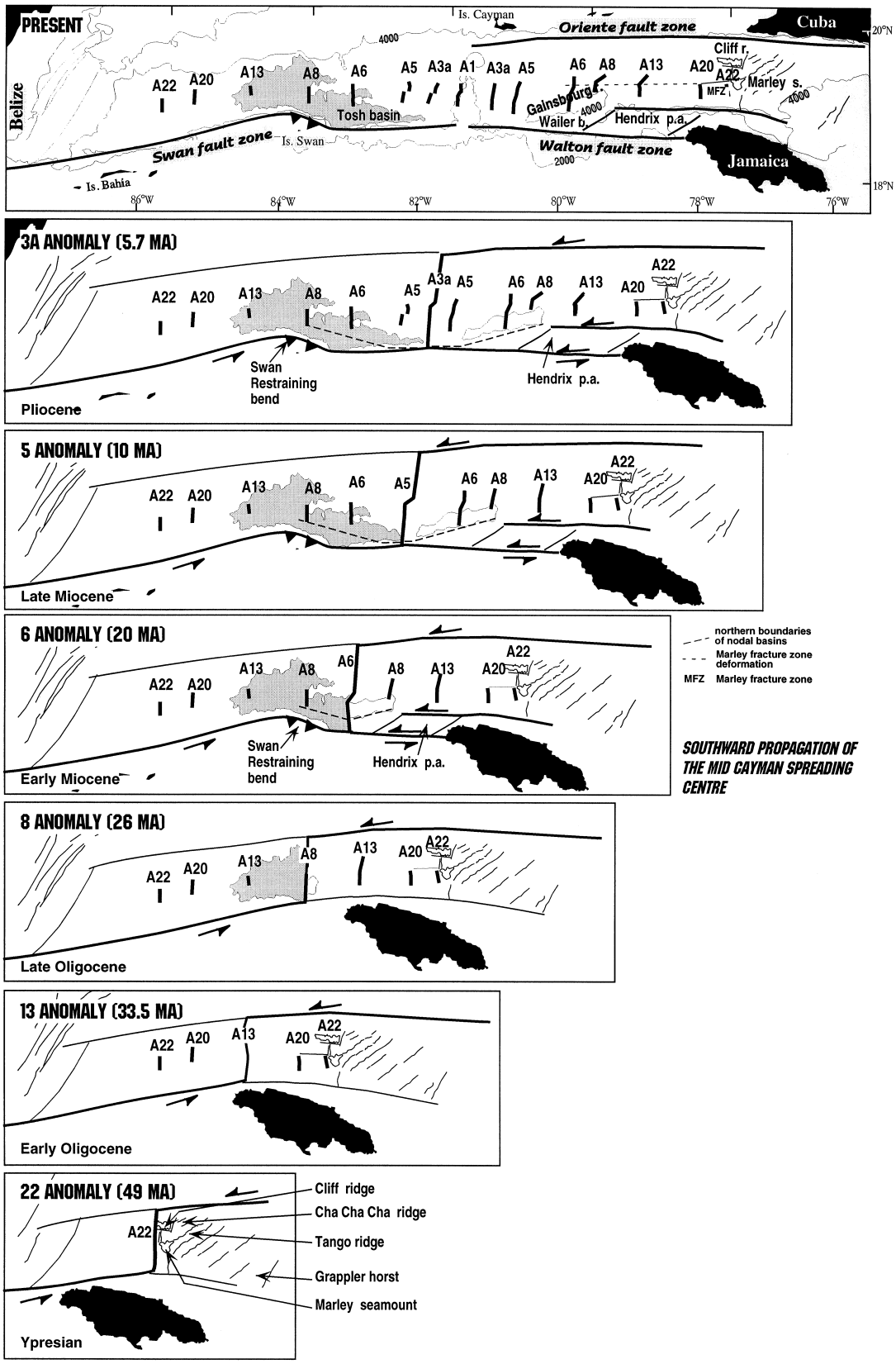

Figure 7. Cayman trough kinematic reconstruction based on our anomaly identifications and on our morphological and structural studies. We have superposed the isochron lines. Note that between anomalies A6 and A8, the spreading ridge propagated southwards, creating a second segment. At the same time, the Swan island restraining bend has been formed, as well as the Hendrix pull-apart, because of the reactivation of the Walton fault zone. The Tosh basin and Gainsbourg ridge are drawn to work out the temporal evolution of these structures. The northern boundary lines of the Tosh and Wailer basins are drawn as dashed lines, as well as the Marley fracture zone (MFZ) along the eastern Cayman trough.

Discussion of the identification of magnetic anomalies

The identification of Rosencrantz *et al.* (1988) put the continent–ocean transition at A20 time (Middle Eocene, 42.5 Ma, Fig. 6a) and that of Ramana *et al.* (1995) at A8 time (Late Oligocene, 26 Ma). A comparison of the Rosencrantz *et al.* (1988) model with ours confirms the importance of the magnetic contamination parameter, which gives computed magnetic anomaly shapes closer to the observed magnetic anomalies (Fig. 6b).

Our model (Fig. 6b) does not explain the high amplitude of A8, although it does retain the 'simple' observation of the anomaly's appearance. The main difference between our interpretation and that of Rosencrantz *et al.* (1988) is the two well-lineated high-amplitude anomalies identified by Rosencrantz *et al.* (1988) as two conjugate A11 and A12 on either side of the fossil ridge and by us as A8–A9–A10 and A11–A12. As anomaly amplitudes are greatly variable on the slow spreading ridge (that is, due to the irregularity of the magmatic activity), our model is preferable because of its simplicity: it suggests a less complex Cayman trough story, without three successive ridge jumps. Both models explain the higher bathymetry east of A6 badly (Figs 5 and 6). The model of Ramana *et al.* (1995) is comparable to ours but does not analyse the magnetic anomaly up to the continent–ocean transition, dating it at A8. Indeed, their two magnetic profiles are not parallel to the spreading direction and cross the boundary between the oceanic and continental crust on the western side of the Oriente fault zone, but not the continent–ocean transition of the Belize continental margin.

The anomaly picks were plotted to produce an isochron map (Fig. 7). Each isochron line represents the old axis geometry at this isochron time within both flanks. We obtain a reconstruction by superposing these isochrons, taking into account tectonic constraints such as transform fault strike, topography of the seafloor and basement, and deformation.

Fig. 7 shows the structural evolution through time resulting from the magnetic anomaly identification. The main result of our reconstruction (Fig. 8) is the propagation towards the south of the ridge axis after A8 time (between A8 and A6), at which point the Cayman trough width increases by about 30 km. Creation of the second segment corresponds to the time of the small spreading rate change. The southwards propagation of the Mid-Cayman spreading centre, from Middle Oligocene (26 Ma) to Early Miocene (20 Ma), results in the development of the Swan islands restraining bend (Figs 2 and 3; Mann *et al.* 1991) and the formation of a 1 km high scarp on the eastern transform fault zone (Fig. 3). Indeed, in the Miocene (A6), the fossil part of the Swan transform fault, called the Walton fault, is reactivated and shows a left-lateral strike-slip displacement, which could explain the formation of the pull-apart basin (Hendrix pull-apart) observed in the bathymetry

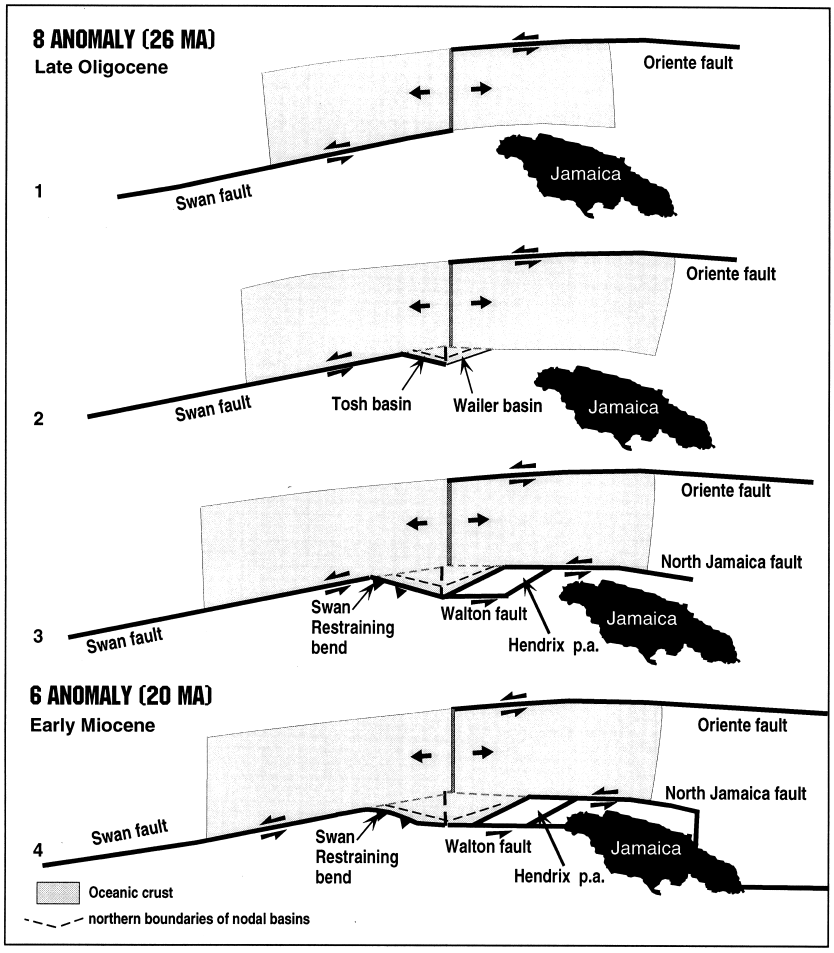

Figure 8. Sketch of the southward progressive growth of the second segment of the Mid-Cayman spreading centre between A8 and A6 times.

west of Jamaica (Figs 2, 3 and 8). The Hendrix pull-apart is located on the northern edge of the Upper Nicaragua rise and limited to the west by the Walton fault bend (Fig. 7). The upper Nicaragua rise consists of Late Cretaceous-aged island arc rocks (Arden 1975) (Fig. 1).

Furthermore, the Gainsbourg ridge and the Tosh basin appear as two contemporaneous but distinct structures, not as the same structure. The Tosh basin has an equivalent structure on the eastern flank, the Wailer basin, located between the Walton fault and the Gainsbourg ridge (Figs 3 and 8). The Gainsbourg ridge was created before A8, in the Early Oligocene, just before the axis propagated southwards. The southern boundary of the ridge is marked by the Wailer basin, the nodal basin of the transform fault zone. On the western flank of the Mid-Cayman spreading centre, the Tosh depression is created, but no ridge formation occurs. The Tosh basin shown in Fig. 7, at A8 time, is arbitrary because it did not extend towards the North so much at this time, but constituted the eastern flank of the nodal basin.

In Fig. 8, a sketch of the southward propagation of the Mid-Cayman spreading centre shows that the northern boundaries of the Tosh and Wailer basins and the Swan–Walton faults bend to form a V-shape, as we previously described in the bathymetry. This seems to correspond to the progressive initiation of the second segment of the spreading centre and its southward propagation (Figs 8 and 9).

Before A6, at the beginning of the Miocene, the Hendrix area was created as an extensional pull-apart basin, contemporaneously with the left-lateral strike-slip displacement of the Walton fault. Since the Miocene, the predominant displacement of Jamaica has been towards the east. Our reconstruction attempts to close the Hendrix pull-apart basin, taking into account the deformation (Fig. 7). The reconstruction presented in Fig. 7 also shows that a tectonic boundary symmetric to the Swan and Oriente faults exists from the inception of the spreading.

In the next stage of the study, an anomaly map of the North Jamaica margin can give us more information about this spreading onset and the interpretation of the area.

MAGNETIC INTERPRETATION OF THE NORTH JAMAICA MARGIN

Magnetic anomaly map

A new magnetic anomaly map has been created for the North Jamaica margin (Fig. 9) from the Seacarib II, Casis I and Wilkes surveys. On it we place the anomaly identifications made along the magnetic profiles in order to extend the interpretation.

The magnetic anomaly map illustrates the ridges striking NNE–SSW in the continental zone (Leroy *et al.* 1996) and anomalies striking NNW–SSE in the oceanic domain (Fig. 9). A large negative magnetic anomaly (−100 nT) extends from Marley seamount to the northeast of the Cha Cha Cha and Tango ridges (Fig. 9). Its western side corresponds to the continent–ocean transition identified by Leroy *et al.* (1996), and its N–S strike is obvious mainly close to Jamaica. This strong anomaly could be the trace of fissure volcanism that started during the Cayman trough opening. The continent–ocean transition is described as narrow and displays several features: basin–fault zone intersections and a ridge formed by the Marley seamount and its northern extension (Leroy *et al.* 1996) (Fig. 9). Note that in the southeastern part of the map, an extension seawards of the Low Layton volcano, described by Leroy *et al.* (1996) on a depth basement map and on land by Pisot (1989), is emphasized by a positive magnetic anomaly of 100 nT located at 18°20′N, 76°30′W (Fig. 9).

Furthermore, north of 19°N, the map shows the effect of the Cliff and Marley fracture zones (Leroy *et al.* 1996) (Fig. 9). Additionally, the trace of the Marley fracture zone can be followed further west, up to the Mid-Cayman spreading ridge. The Marley fracture zone deformation can be seen on the isochron lines in Fig. 7 (eastern A6, A8 and A13) and must have been emphasized by the left-lateral reactivation of the Walton fault in the Miocene (Fig. 7).

Distribution of the magnetization

The magnetic anomaly map described above is a representation of the magnetization distribution of the rocks of the seafloor filtered by the bathymetry. To determine this distribution of magnetization, we have computed a 3-D inversion of the magnetic data (Macdonald *et al.* 1980). First, we made an interpolation of the bathymetric and magnetic data on a grid with knot spacings of 1.1141 km for y (latitude) and 1.0534 km for x (longitude) at the mean latitude of 18°30′N.

The magnetic inversion calculation relies upon several assumptions: magnetized rock layers have a constant thickness fixed at 1 km; the strike of the magnetization vector is constant and corresponds to that of a centred axial dipole; only the sense changes during reversals. Some of these assumptions can be contested. For example, the first limits the study to the oceanic domain and the second does not seem to be verified by the recent studies made on deep boreholes, which indicate that the gabbroic layer may contribute to the observed magnetic anomalies (ODP hole 735B, Kikawa & Pariso 1991). Outside the purely oceanic domain, the results obtained are not entirely accurate due to the initial assumptions.

Fig. 10 shows the magnetization distribution map of the Eastern Cayman zone. We find again the NNE–SSW strike characteristic of the domain of continental blocks. The rifted blocks show a strong magnetization, up to 25 A m^{-1} for the Grappler horst. In the oceanic domain, the positive magnetic anomaly striking NNW–SSE (100 nT, Fig. 9) corresponds to a magnetization of 3 A m^{-1}. Therefore, the amplitude of this anomaly is due to the positive topography. Besides, Marley seamount does not appear clearly on the magnetization distribution map and the values of magnetization in this area (from 2 to 8 A m^{-1}) could correspond to a serpentinized peridotite rock type, which has a magnetization ranging from 2.4 to 8.2 A m^{-1} (Telford *et al.* 1990; Johnson & Pariso 1993). In a continent–ocean transition zone, rocks of this type have been sampled, notably on the west Iberia margin (Boillot *et al.* 1989; Beslier *et al.* 1993; Whitmarsh & Sawyer 1993), but the similarities cannot be confirmed without drilling or near-bottom measurements. The fracture zones already seen on the magnetic anomaly map are apparent in this magnetization distribution map, which also makes the Cliff fracture zone more obvious than the Marley fracture zone (Fig. 10). The Cliff ridge,

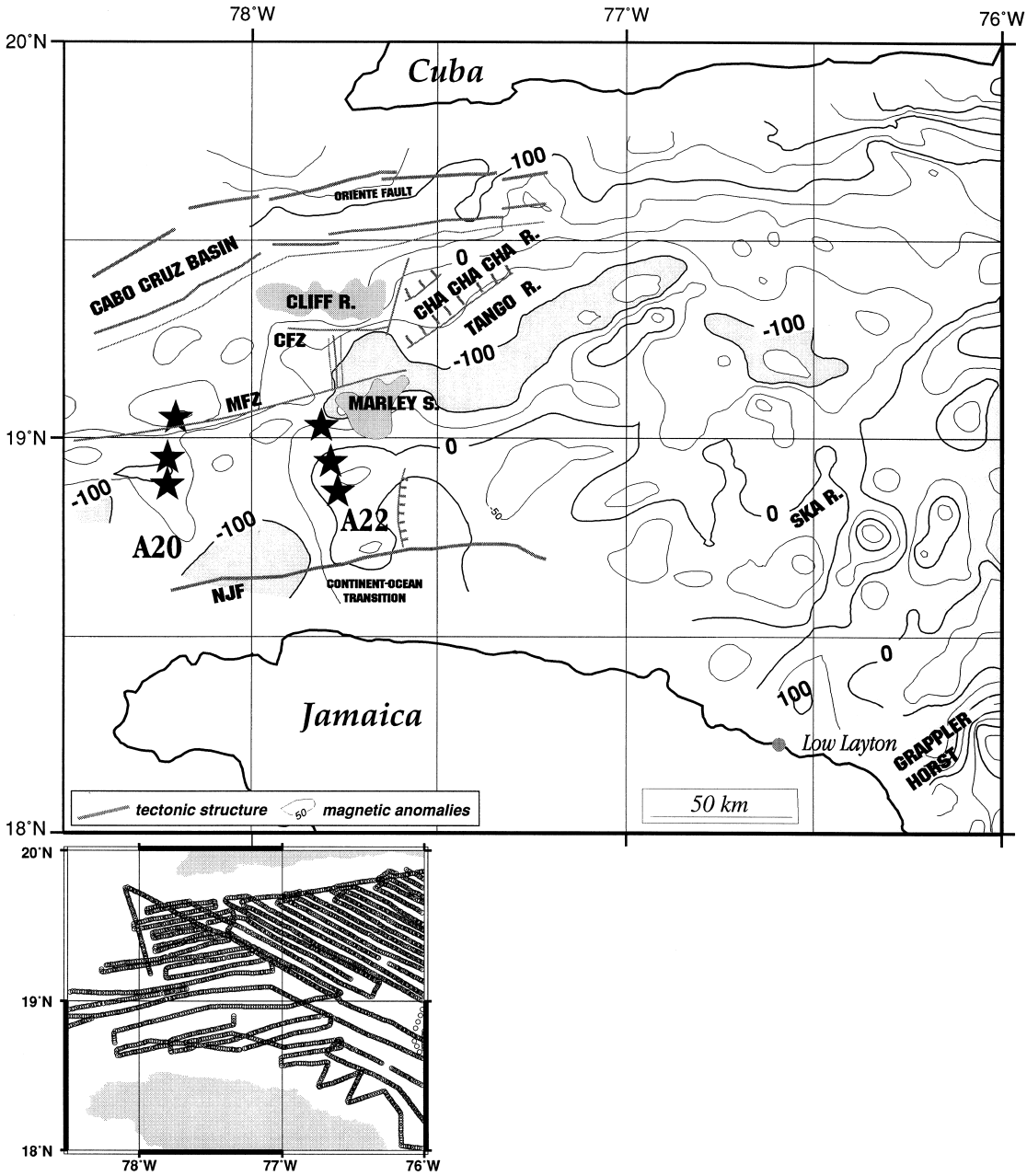

Figure 9. Magnetic anomaly map of the eastern Cayman trough. Contour interval is 50 nT. Note the location of the last magnetic anomaly identified in the oceanic domain and the east–west trend of the Cliff and Marley fracture zones. The continent–ocean transition was dated with our magnetic model. The figure shows the magnetic anomaly contour map and the main structural features. A22 corresponds to the Ypresian (49 Ma). CFZ = Cliff Fracture Zone; MFZ = Marley Fracture zone; NJF = North Jamaica Fault. The inset map displays all existing data used in this area. See text for explanation.

striking E–W, is highly magnetized (15 A m^{-1} average). Such magnetization may correspond to basaltic rocks (Telford *et al.* 1990). A wide reversely magnetized zone (−8 to −19 A m^{-1}) is clearly visible on the last continental Cha Cha Cha ridge and on its associated basin (Fig. 10). This magnetization could correspond to basalts, again related to the rifting. This area extends towards the Oriente deep.

The magnetization distribution in the crust shows the two types of crust and the different strikes: one strike corresponding to the continental domain (NNE–SSW) and the other to the oceanic domain (N–S to NNW–SSE). These observations match the results of the previous structural study from multichannel seismic data (Leroy *et al.* 1996). However, we have to be very careful in interpreting the magnetization results of the continental area.

DISCUSSION

Our magnetic study of the Cayman trough provides supplementary constraints on tectonic and kinematic evolution. The Mid-Cayman spreading centre is an ultraslow spreading ridge with a rate from 7.5–10 mm yr^{-1} (8.5 mm yr^{-1} at present).

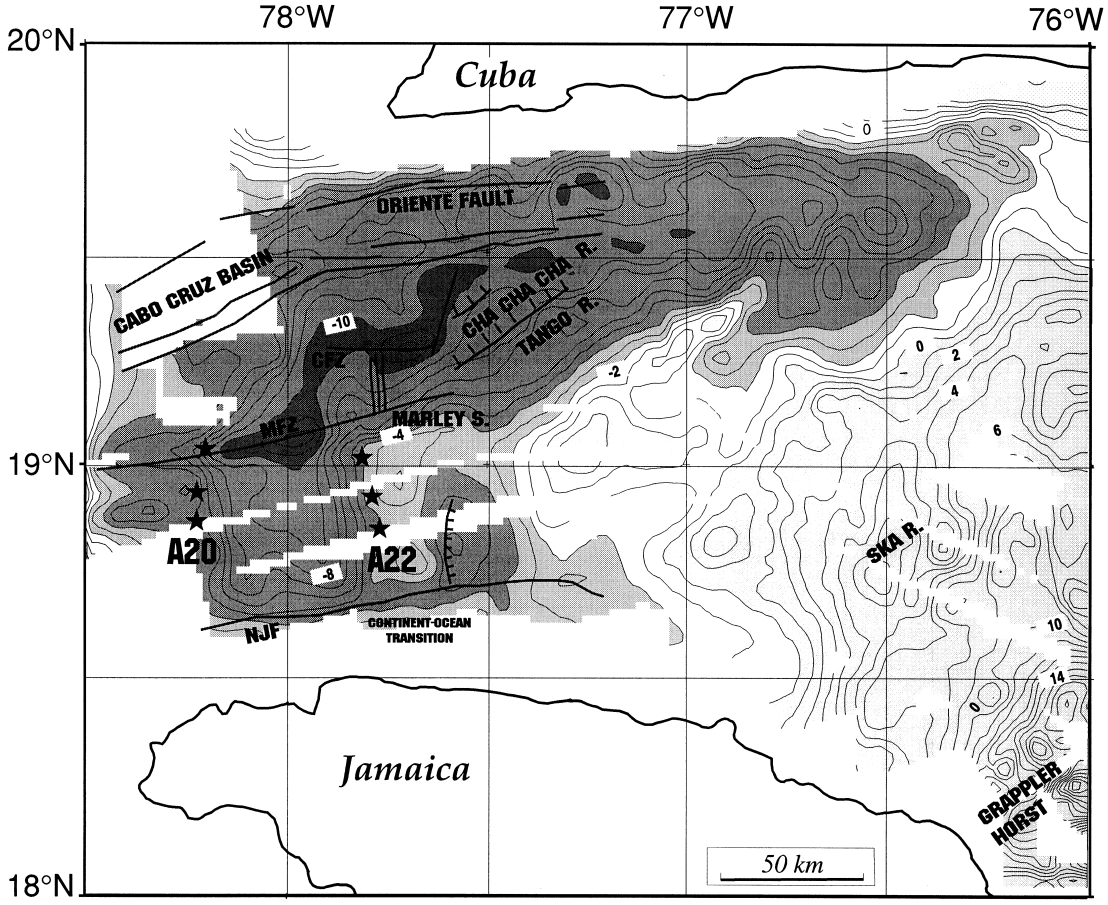

Figure 10. Magnetization distribution map of the Eastern Cayman zone. The continental domain results have to be used with care because of initial assumptions in the inversion calculation (Macdonald *et al.* 1980). The contour interval is 1 A m^{-1}. The values of magnetization on the Marley seamount may correspond to a serpentinized peridotite rock type. The Marley and Cliff fault zones are also visible. CFZ = Cliff Fracture Zone; MFZ = Marley Fracture zone; NJF = North Jamaica Fault. See text for explanation.

The Cayman spreading ridge was composed of a single segment up to A8 and then two segments after A8 time. The second segment was created by the propagation towards the south of the Mid-Cayman spreading centre. This southward propagation of the spreading ridge resulted in a bend of the Swan transform fault and the formation of a restraining bend from the Middle Oligocene to the Early Miocene (Mann *et al.* 1991). These ages correspond to A8 and A6. On Swan island, the exposures of Oligocene terraces are deformed and overlain by undeformed carbonates of post-Early Miocene age (Holcombe *et al.* 1990). On the other side of the axis, on the Walton fault, the structural geometry has undoubtedly been modified during the reactivation of the fossil transform fault during the Miocene epoch (Rosencrantz & Mann 1991). The conjugate structure to the Swan restraining bend can be clearly distinguished on the bathymetric map: the Hendrix rhomboidal area (Fig. 2). Our reconstruction (Fig. 7) shows that this basin may have been formed during the left-lateral strike-slip movement of the Walton fault during the Miocene. Without this reactivation of the inactive Swan transform fault, no pull-apart basin could have been formed at this location. Moreover, the shift of the anomalies at the Marley fracture zone (Fig. 9) was increased by the sinistral displacement of the Walton fault during the Miocene epoch (Fig. 7). The Gainsbourg ridge and the Tosh and Wailer nodal basins bear witness to the southward propagation of the Mid-Cayman spreading centre, leading to the progressive growth of the second segment of the spreading ridge (Figs 7 and 8). Indeed, the propagation of the ridge towards the south is emphasized by the creation of a V-shape in the seafloor topography. The tip of the V indicates the sense of axis propagation (Fig. 8).

The oldest anomaly identified in our model corresponds to A22, which is located on the continent–ocean transition, already identified on multichannel seismic lines (Leroy *et al.* 1996). This A22 corresponds to the onset of the formation of the oceanic crust in the Early Eocene (49 Ma, Ypresian) whereas previous authors (Rosencrantz *et al.* 1988) gave a middle Eocene age (43 Ma, Lutetian). In the eastern corner of Jamaica, the extensional faults striking NW–SE are sealed by the Yellow limestones (Pisot 1989). These limestones form a Ypresian–Lutetian (49–42 Ma) carbonate platform that represents post-rift sedimentation. Thus, our date of the onset of seafloor spreading fits well with the break-up unconformity described on land.

The continent–ocean transition could be made up of magnetized rocks of serpentinized peridotite (8 A m^{-1}), whereas the Cliff ridge could be composed of basaltic material with a very high magnetization (15 A m^{-1}). This configuration is often observed in the slow spreading ridge. In the continental domain, two highly magnetized areas are distinguished along

the Cha Cha Cha, Tango, Grappler and Ska rifted blocks (Fig. 10). The values of the magnetization correspond to a basaltic material that we could consider as being the same as the middle Eocene alkaline volcanism identified in Central Haiti, in the Sierra Maestra (southern Cuba) and in Jamaica. On land, this volcanism shows an alkaline geochemical character and could be related to the rifting.

The results of ODP Leg 165 Site 998 on the Cayman ridge (Fig. 1) describe Eocene calc-alkaline ashes and turbidites (Sigurdsson *et al.* 1997) corresponding to the remains of a subduction zone. However, it appears difficult to reconcile a subduction zone on the south of the Cayman ridge (Fig. 1) with our reconstruction and with other observations. Eocene calc-alkaline material (53 Ma) has been found in Jamaica and is related to an important magmatic episode of island-arc-type that lasted from the Maastrichtian to the Eocene (Pisot 1989). In southern Cuba (Cuban Oriente), the Sierra Maestra is mainly composed of volcanic and volcano-detrital terranes of Late Cretaceous to middle Eocene age (Furrazola-Bermudez 1976; Vila 1984). Their chemistry is calc-alkaline. Thus, the presence of Eocene ashes and turbidites on the Cayman ridge could be related to the calc-alkaline magmatism of Jamaica and Cuba. Our study shows that during Eocene time (A22) the geodynamic framework was a strike-slip system, with the opening of the Cayman trough and not a subduction zone. Thus, we do not agree with the interpretation of the ODP Leg 165 scientific staff. With the complementary bathymetric, structural and magnetic information of our study and with the previous structural work (Leroy *et al.* 1996), we attempt to summarize in the following section a model of the tectonic evolution that confirms and modifies the models of Mann *et al.* (1995) and Gordon *et al.* (1997).

Model of the evolution of the Cayman trough

Our study of the Cayman trough permits us to improve upon the geodynamic model previously proposed for this region (Pindell *et al.* 1988; Calais *et al.* 1989; Pindell & Barrett 1990; Stephan *et al.* 1990; Mann *et al.* 1995; Gordon *et al.* 1997) thanks to the results presented by Leroy *et al.* (1996) and our analyses of bathymetric and magnetic data. The northern boundary of the Caribbean plate moved progressively southwards from the Late Cretaceous to the present. The basic model, presented by Malfait & Dinkelman (1972) and improved by Mann *et al.* (1995) and Gordon *et al.* (1997), emphasizes the progressive collision of Cuba and a subsequent abandonment of fragments of the Caribbean plate that are accreted to the North American plate. The motion of the Caribbean shifts progressively from the north to the east to escape towards a free 'boundary' in the Atlantic ocean (Fig. 11). Thus, the geodynamic evolution of the northern boundary of the Caribbean plate has a tectonic style of oblique arc–continent collision followed by strike-slip faulting.

(a) Late Cretaceous (Fig. 11a)

The initial contact between the North America plate and the eastward-moving Caribbean plate is well documented in the southern part of the Yucatan peninsula. Indeed, in Guatemala (Central America), the synorogenic sedimentation, the northerly vergence of folds, the thrusts and the ophiolitic obduction are Santonian–Campanian–Maastrichtian in age (Rosenfeld 1981; Fourcade *et al.* 1994) (Fig. 11a). This deformation marks the inception of the Cuban arc strike-slip along the Yucatan peninsula. The proto-Caribbean oceanic area allows the Cuban arc system to continue migrating to the northeast towards the Bahamas platform. The magmatic activity recorded at this time is island-arc-type in Cuba, Haiti and Jamaica.

(b) Palaeocene time (Fig. 11b)

Northeastward progression of the arc system is attested by the Cuban arc collision against the Bahamas platform in western Cuba (Gordon *et al.* 1997). Coeval opening of the Yucatan basin occurs along a left-lateral strike-slip fault following the coastline of the Yucatan peninsula (Rosencrantz 1990). In northern Cuba, on the Pinar fault zone, a NW–SE oriented compression was immediately followed by NNE–SSW compression related to the sinistral shear (Gordon *et al.* 1997). The western Cuban arc progression was stopped by the entry of the thicker crust of the Bahamas platform into the subduction zone.

(c) Early Eocene time (Fig. 11c)

The collision migrates to central Cuba. The formation of the Trocha fault accommodates the northeastward relative plate motion. A deformation front occurs to the south along the Cauto depression in southern Cuba.

(d) Ypresian time (Fig. 11d)

The Cayman pull-apart basin opens. The continental break-up begins during the early Eocene (49 Ma, Ypresian). The system cannot advance eastwards and then shifts southwards, initiating the Cauto fault system (Fig. 11d). The eastern boundary of the system is made up of the southern tip of Cuba and part of Hispaniola, which both continue to migrate towards the NNE. The Cauto fault in the previous interpretations (Mann *et al.* 1995; Gordon *et al.* 1997) was never mentioned because previous authors never considered the evolution of the Cuban arc front collision through time along a NW–SE axis. Hereafter, the Cayman trough begins to evolve freely, creating the oceanic crust with an ultraslow spreading rate (7.5 mm yr^{-1}).

Note that the subduction zone in the Cayman trough to the south of the Cayman ridge proposed by Sigurdsson *et al.* (1997) appears to be incompatible with the opening of the Yucatan basin as a pull-apart basin in the Palaeocene, with the Trocha fault activity in the Early Eocene and with the inception of the Cayman trough opening.

(e) Early Oligocene time (Fig. 11e)

The system once again stops in the east, and the Cauto fault is abandoned. The Oriente fault now permits eastward motion of the Caribbean large igneous province along the Pedro–Gonave escarpment. Subduction of the igneous province beneath southwestern Hispaniola now begins and the boundary of the plate evolves progressively southwards. The Neogene shortening causes the formation of an anticline ramp (Mercier de Lépinay 1987). The shortening is due to this oblique convergence.

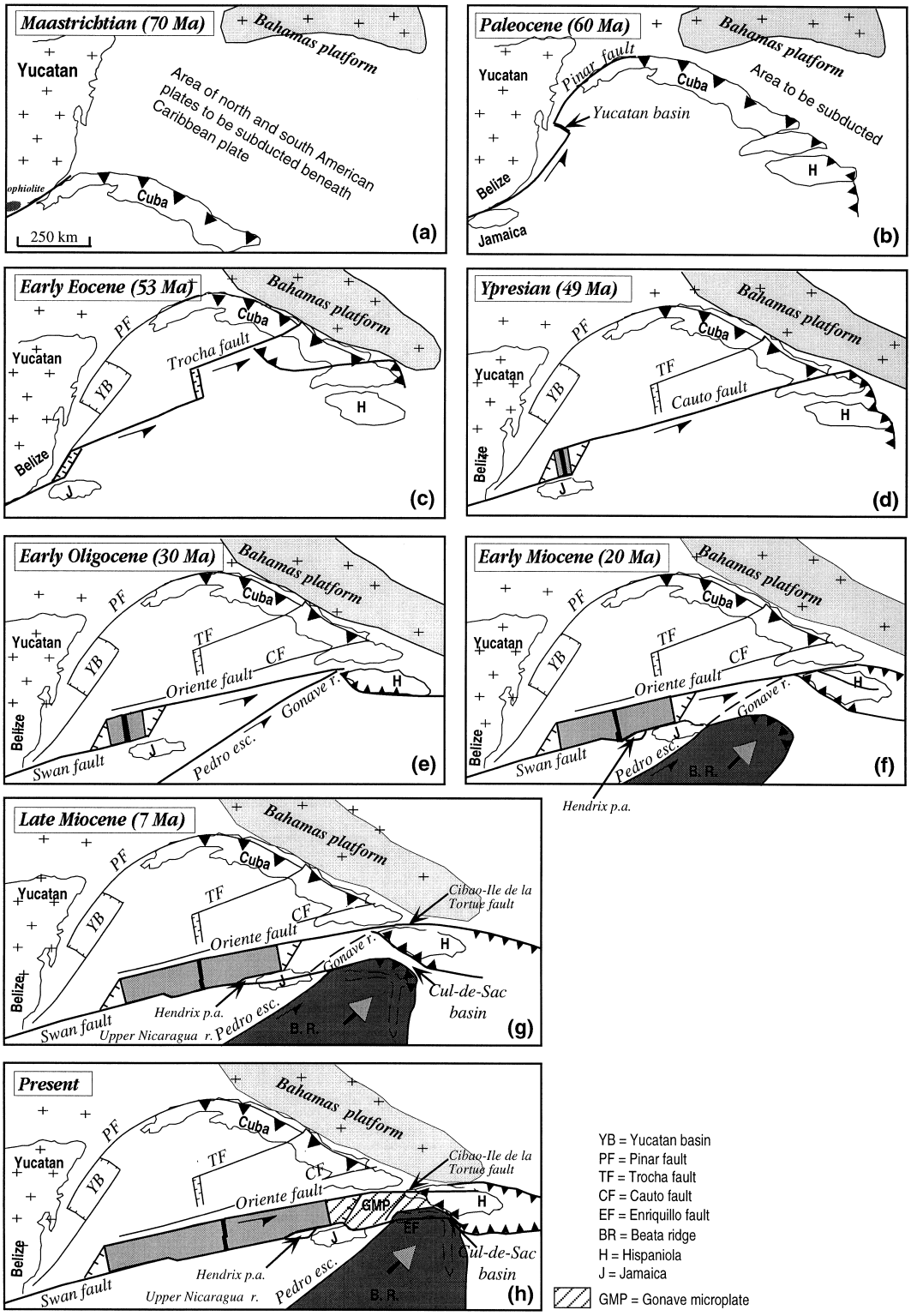

Figure 11. Tectonic setting of the northern boundary of the Caribbean plate from Maastrichtian to Recent times, modified from Pindell & Barrett (1990), Mann *et al.* (1995) and Gordon *et al.* (1997) with the results of this study and that of Leroy *et al.* (1996). See text for discussion.

(f) Late Oligocene, early Miocene (Fig. 11f)

A regional reorganization is completed. Indeed, from the Middle Oligocene, the Mid-Cayman spreading centre propagates progressively southwards, creating a second segment and allowing the formation of the restraining bend of the Swan islands (Mann *et al.* 1991). Transpressive deformation and uplifts form the present topography of the Northern Caribbean domain. The inactive side of the Swan transform fault (Walton fault) becomes active. From eastern Jamaica (Burke *et al.* 1980;

Lewis 1980; Mann *et al.* 1985) to the northern boundary of the Upper Nicaragua rise, the Walton fault activity creates the Hendrix pull-apart basin and the compressive Montego ridges (Leroy *et al.* 1996) (Fig. 1) to the west and north of Jamaica, respectively. Cuba and northern Hispaniola are separated by the transcurrent motion of the Oriente fault. The initiation of this fault explains the difference in movement measured in the Cayman trough (1100 km) and between Cuba and Hispaniola (400 km) (Calais *et al.* 1990).

(g) Late Miocene (Fig. 11g)

The Gonave rise fault is abandoned and the transcurrent motion shifts southwards on the Enriquillo fault in Haiti (Fig. 1), permitting the system to continue to evolve eastwards. The Cayman trough and in particular the Gonave microplate (Rosencrantz & Mann 1991) are related to the Caribbean plate by the Cul-de-Sac basin (Fig. 11g).

(h) Present-day (Fig. 11h)

The final stage of the evolution of the Cayman trough is the Beata ridge collision (Mauffret & Leroy 1999), impeding the strike-slip motion and forcing the convergence to migrate to the Puerto Rico–Bahamas trough (Heezen *et al.* 1985) and to the Cibao–Ile de la Tortue strike-slip fault on the north side of Hispaniola (Fig. 11h).

The history of the Cayman trough is marked by two main tectonic events: (1) the oceanic accretion at A22 (49 Ma) and (2) the reorganization in the Late Oligocene and Early Miocene (A8–A6, 26–20 Ma). These two key epochs are also observed in the global kinematics of the three major tectonic plates bounding the Caribbean plate—the North and South American plates and the Pacific plate. A quantitative analysis of North and South American plate motions (Müller *et al.* 1999) since A34 (83 Ma) agrees with the Cayman trough tectonic history. Indeed, an increase of the N–S movement between the two plates is recorded between A25 (56 Ma, Late Palaeocene) and A21 (47 Ma, Early Eocene), corresponding to the activity period of the different strike-slip faults in Yucatan until the inception of the Cayman trough opening at a slow spreading rate. At A8 (26 Ma, Late Oligocene), the motion between the two plates increases again after slow motion during the Oligocene. Moreover, an increase of the northeastward Pacific plate motion has been recorded at the same time (A21 and A7) by Pardo-Casas & Molnar (1987).

CONCLUSIONS

By studying the magnetic anomalies, the bathymetry and the tectonic structure, we have reached the following conclusions.

(1) The opening of the Cayman trough initiated in Early Eocene time (A22, 49 Ma, Ypresian), consistent with the geology of Jamaica.

(2) Southwards propagation of the spreading ridge occurred in Early Miocene time as well as coeval formation of the Swan restraining bend and reactivation of the Walton fault zone, which formed the Hendrix pull-apart basin.

(3) The northern Caribbean boundary is a good illustration of the tectonic escape that occurred from the Maastrichtian to the present. The final stage was the Beata ridge collision, which impeded strike-slip motion and forced the convergence to migrate into the Puerto Rico Bahamas trough towards a free 'boundary'.

(4) The history of the Cayman trough is directly related to global plate kinematics. Two increases of the convergence rate of the North and South American plates occurred at the two key epochs of the Cayman trough development: oceanic spreading of the trough occurred at 49 Ma, and formation of the Mid-Cayman spreading centre second segment and tectonic reactivation occurred at 26 Ma.

ACKNOWLEDGMENTS

The authors are grateful to C. Rommevaux-Jestin and J. C. Sempéré for the magnetic inversion, to J. Diebold for his helpful comments and to J. Sclater and the Editor for their reviews and improvements to the text. Contribution CNRS-ESA 7072.

REFERENCES

Arden, D.D., 1975. Geology of Jamaica and the Nicaragua rise, in *The Ocean Basins and Margins,* Vol. 3, *The Gulf Of Mexico And The Caribbean,* pp. 617–661, eds Nairn, A.E.M. & Stehli, T.G., Plenum, New York.

Beslier, M.O., Ask, M. & Boillot, G., 1993. Ocean–continent boundary in the Iberia Abyssal Plain from multichannel seismic data, *Tectonophysics,* **218,** 383–394.

Boillot, G., Feraud, G., Recq, M. & Girardeau, J., 1989. 'Undercrusting' by serpentinite beneath rifted margins, *Nature,* **341,** 523–525.

Burke, K., Grippi, J. & Sengor, A.M.C., 1980. Neogene structure in Jamaica and the tectonic style of the northern Caribbean plate boundary zone, *J. Geol.,* **88,** 375–386.

Calais, E. *et al.,* 1989. Evolution paléogéographique et structurale du domaine caraïbe du Lias à l'Actuel: 14 étapes pour 3 grandes périodes, *C. R. Acad. Sci. Paris,* **309,** 1437–1444.

Calais, E., Mercier de Lepinay, B. & Bethoux, N., 1990. Relations contraintes/cinématique le long d'un décrochement lithosphérique actif: la limite de plaques nord caraïbe de Cuba à Hispaniola, *C. R. Acad. Sci. Paris,* **311,** 1259–1266.

Cande, S.C. & Kent, D.V., 1995. Revised calibration of the geomagnetic polarity timescale for the Late Cretaceous and the Cenozoic, *J. geophys. Res.,* **100,** 6093–6095.

CAYTROUGH, 1979. Geological and geophysical investigations of the Mid-Cayman Rise spreading centre: initial results and observations, in *Deep Drilling Results in the Atlantic Ocean: Oceanic Crust, Maurice Ewing Series,* Vol. 2, pp. 66–93, eds Talwani, M. *et al.,* AGU, Washington.

Fourcade, E., Mendez, J., Azéma, J., Cros, P., De Wever, P., Duthou, J.L., Romero, J.E. & Michaud, F., 1994. Age présantonien-campanien de l'obduction des ophiolites du Guatemala, *C. R. Acad. Sci. Paris, serie T,* **318,** 527–533.

Furrazola-Bermudez, G., 1976. Nuevos dateos de la estratigrafia del Cretacico superior de la Sierra Maestra occidental, *Revista Mineria En Cuba, Ano,* **2,** 3.

Gordon, M., Mann, P., Caceres, D. & Flores, R., 1997. Cenozoic tectonic history of the North America–Caribbean plate boundary zone in western Cuba, *J. geophys. Res.,* **102,** 10 055–10 082.

Heezen, B.C., Nesteroff, W.D., Rawson, M. & Freeman-Lynde, R.P., 1985. Visual evidence for subduction in the western Puerto rico trench, in *Symp. 'Géodynamique Des Caraïbes',* Vols 5–8, pp. 287–304, ed. Mascle, A., Technip, Paris.

Holcombe, T.L. & Sharman, G.F., 1983. Post-Miocene Cayman Trough evolution: a speculative model, *Geology,* **11,** 714–717.

Holcombe, T.L., Vogt, P.R. & Matthews, J.E., 1973. Evidence for sea-floor spreading in the Cayman Trough, *Earth planet. Sci. Lett.,* **20,** 357–371.

Holcombe, T.L., Ladd, J.W., Westbrook, G., Edgar, T. & Bowland, C.L., 1990. Caribbean marine geology and basins of the plate interior, in *The Geology of North America,* Vol. H, *The Caribbean Region (A Decade of North American Geology),* pp. 231–260, eds Dengo, G. & Case, J.E., Geol. Soc. Am., Boulder, CO.

IAGA, 1985. Division I working group, International geomagnetic reference field 1985, *J. Geomag. Geoelectr.,* **37,** 1157.

Johnson, H.P. & Pariso, J.E., 1993. Variations in oceanic magnetization: systematic changes in the last 160 Million years, *J. geophys. Res.,* **98,** 435–445.

Jordan, T.H., 1975. The present-day motions of the Caribbean plate, *J. geophys. Res.,* **80,** 4433–4439.

Kent, D.V. & Gradstein, F.M., 1986. A Jurassic to recent chronology, in *The Western North Atlantic Region,* Vol. M, pp. 45–50, eds Vogt, P.R. & Tucholke, B.E., Geol. Soc. Am., Boulder, CO.

Kikawa, E. & Pariso, J., 1991. Magnetic properties of Gabbros from hole 735B, Southwest Indian ridge, in *Proc. ODP, Scientific Results,* Vol. 118, pp. 285–307, eds Von Herzen, R.P. *et al.,* US Govt Printing Office, Washington, DC.

Ladd, J., Holcombe, T.L., Westbrook, G.K. & Edgar, N.T., 1990. Caribbean marine geology; active margins of the plate boundary, in *the Geology of North America,* Vol. H, *The Caribbean Region (A Decade of North American Geology),* pp. 261–290, eds Dengo, G. & Case, J.E., Geol. Soc. Am, Boulder, CO.

Langel, R.A., 1988. International geomagnetic reference field revision 1987, *EOS, Trans. Am. geophys. Un.,* **69,** 557–558.

Le Douaran, S. & Francheteau, J., 1981. Axial depth anomalies from 10 to 50° north along the Mid-Atlantic Ridge: correlation with other mantle properties, *Earth planet. Sci. Lett.,* **54,** 29–47.

Leroy, S., 1995. Structure et origine de la plaque Caraïbe, implications géodynamiques, *Doctorat d'Université thesis,* Université P & M Curie, Paris.

Leroy, S., Mercier de Lepinay, B., Mauffret, A. & Pubellier, M., 1996. Structure and tectonic evolution of the Eastern Cayman Trough (Caribbean Sea) from multichannel seismic data, *Am. Assoc. petrol. Geol. Bull.,* **80,** 222–247.

Lewis, J.F., 1980. Cenozoic tectonic evolution and sedimentation in Hispaniola, in *Mem. Trans. 9a Conf. Geol. Caribe: Santo Domingo, Republica Dominicana,* pp. 65–73.

Macdonald, K.C. & Holcombe, T.L., 1978. Inversion of magnetic anomaly and sea-floor spreading in the Cayman Trough, *Earth planet. Sci. Lett.,* **40,** 407–414.

Macdonald, K.C., Miller, S.P., Huestie, S.P. & Spiess, F.N., 1980. Three-dimensional modeling of a magnetic reversal boundary from inversion of deep-tow measurements, *J. geophys. Res.,* **85,** B7.

Malfait, B.T. & Dinkelman, M.G., 1972. Circum-Caribbean tectonic and igneous activity and the evolution of the Caribbean plate, *Geol. Soc. Am. Bull.,* **83,** 251–272.

Mann, P., Draper, G. & Burke, K., 1985. Neotectonics of a strike-slip restraining bend system, Jamaica, in *Strike-Slip Deformation, Basin Formation and Sedimentation,* eds Biddle, K.T. & Christie-Blick, N., *SEPM Spec. Publ.,* **37,** 211–226.

Mann, P., Tyburski, S.A. & Rosencrantz, E., 1991. Neogene development of the Swan Islands restraining bend complex, Caribbean Sea, *Geology,* **19,** 823–826.

Mann, P., Taylor, F.W., Lawrence Edwards, R. & Teh-Lung Ku, 1995. Actively evolving microplate formation by oblique collision and sideways motion along strike-slip faults: an example from the northeastern Caribbean plate margin, *Tectonophysics,* **246,** 1–69.

Mauffret, A. & Leroy, S., 1999. Neogene intraplate deformation of the Caribbean plate at the Beata Ridge, in *Caribbean Basins, Sedimentary Basins of the World,* Vol. 4, pp. 627–669, ed Mann, P., Elsevier, Amsterdam.

Mercier de Lépinay, B., 1987. Evolution de la bordure nord-caraïbe: l'exemple de la transversale d'Hispaniola, *Doctorat d'Etat thesis,* Université P. et M. Curie, Paris.

Mocquet, A. & Aggarwal, Y.P., 1983. Seismic slip rates in the Greater and Lesser Antilles; implications for the present-day motion of the Caribbean plate relative to North America, *EOS, Trans. Am. geophys. Un.,* **64,** 832.

Molnar, P. & Sykes, L., 1969. Tectonics of the Caribbean and Middle America regions from focal mechanism and seismicity, *Bull. Geol. Soc. Am.,* **80,** 1639–1684.

Müller, R.D., Royer, J.Y., Cande, S.C., Roest, W.R. & Maschenkov, S., 1999. New constraints on the Late Cretaceous/Tertiary plate tectonic evolution of the Caribbean, in *Caribbean Basins, Sedimentary Basins of the World,* Vol. 4, pp. 33–59, ed. Mann, P., Elsevier, Amsterdam.

Pardo-Casas, F. & Molnar, P., 1987. Relative motion of the Nazca (Farallon) and south American plates since Late Cretaceous time, *Tectonics,* **3,** 233–248.

Pariso, J., Rommevaux, C. & Sempéré, J.C., 1996. Three-dimensional inversion of marine magnetic anomalies: implications for crustal accretion along the Mid-Atlantic Ridge (28°–31°30′N), *Mar. geophys. Res.,* **18,** 85–101.

Parsons, B. & Sclater, J.G., 1977. An analysis of the variation of ocean floor bathymetry and heat flow with age, *J. geophys. Res.,* **82,** 803–827.

Patriat, P., 1987. Reconstitution de l'évolution du système de dorsales de l'Océan Indien par les méthodes de la cinématique des plaques, *Territoire des Terres Australes et Antartiques Françaises,* TAAF, Paris.

Perfit, M.R., 1977. Petrology and geochemistry of mafic rocks from the Cayman trench: evidence for spreading, *Geology,* **5,** 105–110.

Pindell, J.L. & Barrett, S.F., 1990. Geological Evolution of the Caribbean Region, in *the Geology of North America,* Vol. H, *The Caribbean Region (A Decade of North American Geology),* pp. 405–432, eds Dengo, G. & Case, J.E., Geol. Soc. Am., Boulder, CO.

Pindell, J.L., Cande, S.C., Pitmann, W.C., Rowley, D.B., Dewey, J.F., Labrecque, J.L. & Haxby, W., 1988. A plate-kinematic framework for models of Caribbean evolution, in *Mesozoic and Cenozoic Plate Reconstruction,* eds Scotese, C.R. & Sager, W.W., *Tectonophysics,* **155,** 121–138.

Pisot, N., 1989. Synthèse lithostratigraphique et tectonique de l'ile de la Jamaïque et de sa marge septentrionale, *Université thesis,* Nice.

Ramana, M.V., Ramprasad, T., Grahm, B., Welsh, R. & Pathak, M.C., 1995. Magnetic studies in the Cayman trough, Caribbean sea, *Carib. Mar. Stud.,* **4,** 30–38.

Rommevaux, C., 1994. Etude gravimétrique et magnétique de l'évolution de la segmentation des dorsales lentes, *Doctorat thesis,* Paris VII.

Rosencrantz, E., 1990. Structure and tectonics of the Yucatan basin, Caribbean sea, as determined from seismic reflection studies, *Tectonics,* **9,** 1037–1059.

Rosencrantz, E. & Mann, P., 1991. SeaMarc II mapping of transform faults in the Cayman Trough, Caribbean Sea, *Geology,* **19,** 600–693.

Rosencrantz, E. & Sclater, J.C., 1986. Depth and age in the Cayman Trough, *Earth. planet. Sci. Lett.,* **79,** 133–144.

Rosencrantz, E., Sclater, J.C. & Ross, M.L., 1988. Age and spreading history of the Cayman Trough as determined from depth, heat flow and magnetic anomalies, *J. geophys. Res.,* **93,** 2141–2157.

Rosenfeld, J.H., 1981. *The Santa Cruz Ophiolite, Guatemala, Central America,* Amoco, Houston.

Sclater, J.G. & Francheteau, J., 1970. The implications of terrestrial heat flow observations on current tectonic and geochemical models of the crust and upper mantle of the earth, *Geophys. J. R. astr. Soc.,* **20,** 509.

Sigurdsson, H., Leeckie, R.M. & Acton, G.D., 1997. Caribbean volcanism, Cretaceous/Tertiary impact and ocean-climate history: synthesis of leg 165, in *Init. Rept, Proc. ODP,* pp. 377–400, ODP, College Station, TX.

Sloan, H. & Patriat, P., 1992. Kinematics of the North American–African plate boundary between 28° and 29° N during the last 10 My: evolution of the axial geometry and spreading rate and direction, *Earth planet. Sci. Lett.,* **113,** 323–341.

Smith, D.K. & Cann, J.R., 1990. Hundreds of small volcanoes on the median valley floor of the Mid-Atlantic Ridge at 24–30°N, *Nature,* **348,** 152–155.

Stephan, J.F. *et al*., 1990. Paleogeodynamic maps of the Caribbean: 14 steps from Lias to Present, *Bull. Soc. géol. Fr.,* **6,** 915–919.

Stroup, J.B. & Fox, P.J., 1981. Geologic investigations in the Cayman trough: evidence for thin oceanic crust along the Mid-Cayman Rise, *J. Geol.,* **89,** 395–420.

Sykes, L.R., Mccann, W.R. & Kafka, A.L., 1982. Motion of Caribbean Plate during last 7 millions years and implications for earlier Cenozoic movements, *J. geophys. Res.,* **87,** 10 656–10 676.

Telford, W.M., Geldart, L.P. & Sheriff, R.E., 1990. *Applied Geophysics,* Cambridge University Press, Cambridge.

Tisseau, J. & Patriat, P., 1981. Identification des anomalies magnétiques sur les dorsales à faible taux d'expansion: méthode des taux fictifs, *Earth planet. Sci. Lett.,* **52,** 381–396.

Vila, J.M., 1984. Observations sur le Paléogène de la Sierra Maestra près de Santiago de Cuba, *10ème Réun. Sci. Terre,* p. 544, BRGM, Bordeaux.

Wadge, G. & Dixon, T.H., 1984. A geological interpretation of seasat-Sar imagery of Jamaica, *J. Geol.,* **92,** 561–581.

Whitmarsh, R.B. & Sawyer, D.S., 1993. Upper mantle drilling in the ocean-continent transition west of Iberia, *Terra Nova,* **5,** 327–331.